Supplement of Biogeosciences, 15, 7299–7313, 2018
https://doi.org/10.5194/bg-15-7299-2018-supplement

Biogeosciences Open Access EGU

Supplement of

Evolution of ^{231}Pa and ^{230}Th in overflow waters of the North Atlantic

Feifei Deng et al.

Correspondence to: Feifei Deng (feifei.deng@earth.ox.ac.uk)

S1. Data of water-column ^{231}Pa, ^{230}Th and ^{232}Th concentrations, and $^{231}Pa/^{230}Th$ ratios along GEOVIDE section and details of correction

Table S1 Water-column ^{231}Pa, ^{230}Th and ^{232}Th concentrations, and $^{231}Pa/^{230}Th$ ratios along GEOVIDE section

Station	Depth	^{231}Pa	$^{231}Pa_{corr}$	$^{231}Pa_{corr}$	2se	^{230}Th	^{230}Th	$^{230}Th_{corr}$	2se	^{232}Th	^{232}Th	2se	$^{231}Pa/^{230}Th$	2se
	m	fg/kg	fg/kg	µBq/kg		fg/kg	fg/kg	µBq/kg		pg/kg	pmol/kg			
1	3445.3	2.270	2.269	3.96	0.17									
40.33°N	2955.3	2.465	2.463	4.30	0.22									
10.04°W	2465.8	1.988	1.982	3.46	0.22	9.00	8.83	6.72	0.20	52.33	0.2248	0.0046	0.516	0.036
	1974.9	1.592	1.588	2.77	0.19	5.64	5.50	4.18	0.17	43.47	0.1867	0.0036	0.663	0.053
	1385.3	1.522	1.517	2.65	0.23	3.43	3.28	2.50	0.14	44.96	0.1931	0.0041	1.061	0.108
	1039.6	1.176	1.170	2.04	0.20	3.48	3.29	2.50	0.20	59.80	0.2568	0.0049	0.818	0.105
	495.6	0.861	0.853	1.49	0.22	3.67	3.43	2.61	0.16	72.77	0.3125	0.0058	0.571	0.090
	246.9	0.635	0.624	1.09	0.18	2.79	2.47	1.88	0.14	99.60	0.4278	0.0098	0.581	0.104
	49.6	0.641	0.623	1.09	0.20	2.84	2.29	1.74	0.18	171.16	0.7351	0.0133	0.625	0.132
	4.7	0.238	0.210	0.37	0.08	3.93	3.11	2.36	0.09	255.90	1.0991	0.0186	0.155	0.033
13	5330.4	2.093	1.880	3.28	0.24	8.69	8.62	6.56	6.56	22.79	0.0979	0.0017	0.501	0.039
41.38°N	5263.1	2.421	2.178	3.80	0.26	12.66	12.55	9.55	9.55	33.12	0.1422	0.0022	0.398	0.028
13.89°W	5194.3	2.751	2.747	4.80	0.24	15.80	15.67	11.92	11.92	39.61	0.1701	0.0033	0.403	0.023
	4903.9	2.013	2.009	3.51	0.15	14.79	14.68	11.17	11.17	35.27	0.1515	0.0031	0.314	0.016
	4417.8	2.627	2.624	4.58	0.24	11.16	11.07	8.42	8.42	28.70	0.1233	0.0026	0.545	0.033
	3444	2.399	2.396	4.19	0.14	8.15	8.08	6.14	6.14	22.33	0.0959	0.0022	0.681	0.031
	2464.7	1.569	1.565	2.73	0.26	5.77	5.67	4.31	4.31	30.57	0.1313	0.0028	0.634	0.066
	1187.3	0.869	0.865	1.51	0.12	3.24	3.12	2.38	2.38	37.16	0.1596	0.0032	0.637	0.065
	989.1	1.239	1.234	2.16	0.15	4.16	4.03	3.06	3.06	41.38	0.1777	0.0035	0.704	0.063
	248.4	0.602	0.602	1.05	0.11									
	148.5	0.525	0.525	0.92	0.13									
	29.7	0.508	0.507	0.89	0.11	0.44	0.43	0.32	0.15	5.60	0.0241	0.0015	2.736	1.315
	4.3	0.330	0.330	0.58	0.08	0.28	0.26	0.19	0.14	6.70	0.0288	0.0014	2.968	2.154

Station	Depth	^{231}Pa	^{231}Pa	^{231}Pa$_{corr}$	2se	^{230}Th	^{230}Th	^{230}Th$_{corr}$	2se	^{232}Th	^{232}Th	2se	^{231}Pa/^{230}Th	2se
	m	fg/kg	fg/kg	µBq/kg		fg/kg	fg/kg	µBq/kg		pg/kg	pmol/kg			
21	4514.9	2.605	2.603	4.55	0.15	6.09	6.03	4.58	0.19	20.99	0.0902	0.0017	0.992	0.052
46.54°N	4475	2.404	2.401	4.20	0.18	6.21	6.13	4.66	0.28	25.11	0.1079	0.0025	0.900	0.066
19.67°W	4426.3	2.413	2.411	4.21	0.17	5.76	5.70	4.33	0.14	19.57	0.0841	0.0017	0.972	0.051
	4279.6	2.497	2.495	4.36	0.18	5.91	5.85	4.45	0.19	20.48	0.0880	0.0018	0.980	0.059
	3929.3	2.081	2.079	3.63	0.17	5.47	5.41	4.11	0.16	20.11	0.0864	0.0016	0.884	0.053
	3443.3	1.930	1.928	3.37	0.20	4.63	4.57	3.47	0.14	18.16	0.0780	0.0015	0.970	0.070
	2268.9	1.114	1.114	1.95	0.22	5.16	5.06	3.85	0.17	30.49	0.1309	0.0021	0.506	0.060
	1482.7	0.995	0.993	1.73	0.12	2.48	2.39	1.82	0.14	26.83	0.1152	0.0016	0.953	0.097
	788.4	0.873	0.871	1.52	0.14	1.31	1.23	0.93	0.16	25.41	0.1092	0.0018	1.628	0.312
	445.5	0.679	0.676	1.18	0.14	2.18	2.05	1.56	0.14	39.91	0.1714	0.0023	0.756	0.115
	246.9	0.595	0.592	1.03	0.11	1.64	1.53	1.17	0.13	33.41	0.1435	0.0019	0.886	0.139
	98.1	0.607	0.603	1.05	0.14	1.32	1.23	0.93	0.12	28.01	0.1203	0.0019	1.129	0.209
	13.9	0.536	0.532	0.93	0.15					10.81	0.0464	0.0015		
	3.7	0.522	0.519	0.91	0.14					7.95	0.0342	0.0014		
26	4116.3	1.162	1.158	2.02	0.18	3.43	3.29	2.50	0.17	42.15	0.1810	0.0035	0.808	0.088
50.28°N	2758.5	0.813	0.807	1.41	0.15	3.04	2.85	2.17	0.14	57.40	0.2465	0.0047	0.650	0.081
22.60°W	1973.5	0.745	0.739	1.29	0.13	2.83	2.65	2.01	0.16	56.40	0.2422	0.0045	0.642	0.081
	989.1	0.695	0.695	1.22	0.11									
	296.7	0.503	0.503	0.88	0.10									
	74.4	0.408	0.407	0.71	0.12	0.67	0.62	0.47	0.17	13.57	0.0583	0.0018	1.498	0.603

Station	Depth	^{231}Pa	^{231}Pa	^{231}Pa$_{corr}$	2se	^{230}Th	^{230}Th	^{230}Th$_{corr}$	2se	^{232}Th	^{232}Th	2se	^{231}Pa/^{230}Th	2se
	m	fg/kg	fg/kg	µBq/kg		fg/kg	fg/kg	µBq/kg		pg/kg	pmol/kg			
32	3218.7	0.973	0.968	1.69	0.15	5.49	5.35	4.07	0.15	43.48	0.1867	0.0023	0.416	0.039
55.51°N	3218.5	0.984	0.982	1.72	0.12	1.68	1.63	1.24	0.14	15.25	0.0655	0.0016	1.387	0.184
26.71°W	3049.9	1.131	1.129	1.97	0.11	3.27	3.21	2.44	0.13	20.44	0.0878	0.0016	0.809	0.063
	2949.6	1.076	1.075	1.88	0.17	1.74	1.70	1.29	0.13	12.96	0.0557	0.0014	1.456	0.198
	2854.3	1.004	1.002	1.75	0.20	2.65	2.60	1.97	0.17	16.46	0.0707	0.0016	0.887	0.128
	2610.4	1.109	1.108	1.94	0.13	1.82	1.78	1.35	0.14	12.01	0.0516	0.0016	1.429	0.179
	2218.8	0.843	0.842	1.47	0.14	1.30	1.26	0.96	0.13	11.46	0.0492	0.0015	1.533	0.261
	1676.9	1.200	1.199	2.09	0.14	0.87	0.84	0.64	0.12	9.00	0.0387	0.0014	3.261	0.661
	1185.5	1.087	1.082	1.89	0.14	3.58	3.45	2.62	0.15	40.46	0.1738	0.0022	0.721	0.066
	890.5	0.872	0.869	1.52	0.14	1.64	1.55	1.18	0.13	29.00	0.1246	0.0018	1.289	0.187
	445.3	0.944	0.939	1.64	0.14	2.91	2.76	2.10	0.15	46.20	0.1984	0.0026	0.781	0.086
	222.9	0.568	0.564	0.99	0.12	1.70	1.57	1.20	0.13	39.69	0.1705	0.0022	0.824	0.135
	98.9	0.553	0.550	0.96	0.25	6.65	6.56	4.99	0.16	27.70	0.1190	0.0018	0.193	0.050
	29.5	0.613	0.610	1.07	0.27	5.50	5.41	4.12	0.16	27.73	0.1191	0.0019	0.259	0.067
	5.8	0.584	0.583	1.02	0.14					9.92	0.0426	0.0015		
38	1338.1	1.604	1.602	2.80	0.22	1.62	1.57	1.20	0.15	16.07	0.0690	0.0020	2.341	0.338
58.84°N	1303.6	1.336	1.333	2.33	0.11	3.34	3.25	2.47	0.20	29.18	0.1253	0.0026	0.943	0.087
31.27°W	1234.5	1.088	1.085	1.90	0.11	3.42	3.33	2.53	0.15	28.39	0.1219	0.0026	0.748	0.064
	1084	0.863	0.860	1.50	0.10	3.64	3.54	2.69	0.19	31.67	0.1360	0.0027	0.558	0.053
	494.2	1.621	1.616	2.82	0.25	3.16	3.03	2.30	0.16	39.87	0.1712	0.0033	1.226	0.137
	198.4	1.258	1.253	2.19	0.12	3.12	2.97	2.26	0.14	46.64	0.2003	0.0037	0.969	0.081
	108.7	1.274	1.269	2.22	0.19	2.78	2.65	2.01	0.14	42.89	0.1842	0.0036	1.102	0.121
	20.3	0.836	0.835	1.46	0.13	0.84	0.80	0.61	0.13	11.88	0.0510	0.0016	2.389	0.566
	5.3	1.230	1.228	2.15	0.25	0.80	0.76	0.58	0.15	11.59	0.0498	0.0016	3.719	1.055

Station	Depth	^{231}Pa	^{231}Pa	^{231}Pa$_{corr}$	2se	^{230}Th	^{230}Th	^{230}Th$_{corr}$	2se	^{232}Th	^{232}Th	2se	^{231}Pa/^{230}Th	2se
	m	fg/kg	fg/kg	µBq/kg		fg/kg	fg/kg	µBq/kg		pg/kg	pmol/kg			
44	2918.9	0.839	0.837	1.46	0.17	2.40	2.33	1.77	0.13	22.85	0.0981	0.0022	0.827	0.112
59.62°N	2878.5	0.875	0.873	1.52	0.15	2.50	2.42	1.84	0.14	24.44	0.1050	0.0023	0.829	0.102
38.95°W	2829	0.723	0.723	1.26	0.22									
	2681.9	0.651	0.649	1.13	0.24	2.65	2.57	1.96	0.15	25.27	0.1085	0.0024	0.580	0.129
	2561	1.164	1.161	2.03	0.23	4.87	4.78	3.64	0.17	26.47	0.1137	0.0025	0.557	0.069
	2216.6	0.910	0.906	1.58	0.26	6.18	6.08	4.63	0.18	31.25	0.1342	0.0028	0.342	0.058
	1776	1.416	1.412	2.47	0.39	5.87	5.75	4.37	0.15	39.66	0.1704	0.0032	0.564	0.090
	1382.5	1.186	1.182	2.07	0.27	5.85	5.72	4.35	0.15	41.00	0.1761	0.0034	0.475	0.065
	1087.5	0.795	0.790	1.38	0.18	3.83	3.70	2.81	0.15	40.73	0.1749	0.0033	0.491	0.071
	593.2	1.116	1.111	1.94	0.36	4.28	4.13	3.14	0.16	46.81	0.2010	0.0038	0.618	0.118
	297.3	1.083	1.078	1.88	0.20	4.10	3.97	3.02	0.22	42.29	0.1816	0.0036	0.625	0.081
	78.8	0.929	0.925	1.62	0.19	3.44	3.31	2.52	0.14	39.69	0.1705	0.0033	0.641	0.082
	25.5	0.998	0.997	1.74	0.16	1.37	1.32	1.00	0.15	16.50	0.0709	0.0019	1.737	0.297
	5.5	0.722	0.720	1.26	0.33	1.31	1.27	0.96	0.12	14.99	0.0644	0.0018	1.307	0.380
60	1710.9	0.844	0.841	1.47	0.07	3.77	3.67	2.79	0.16	31.42	0.1349	0.0031	0.526	0.039
59.80°N	1652.6	0.881	0.878	1.53	0.07	4.03	3.92	2.98	0.16	33.28	0.1429	0.0032	0.514	0.036
42.01°W	1603.1	0.845	0.842	1.47	0.07	4.10	3.99	3.04	0.24	33.74	0.1449	0.0032	0.485	0.045
	1481.2	0.813	0.809	1.41	0.07	4.19	4.08	3.10	0.17	33.94	0.1458	0.0032	0.455	0.034
	989.7	1.087	1.082	1.89	0.08	5.29	5.15	3.91	0.20	45.60	0.1958	0.0040	0.483	0.031
	495.5	0.911	0.906	1.58	0.16	3.69	3.56	2.71	0.14	39.63	0.1702	0.0033	0.585	0.064
	247.9	0.851	0.847	1.48	0.23	3.16	3.03	2.30	0.14	40.61	0.1744	0.0034	0.643	0.109
	99.1	0.826	0.822	1.44	0.20	2.34	2.23	1.69	0.13	34.75	0.1492	0.0029	0.849	0.134
	19.5	0.887	0.885	1.55	0.32	1.36	1.30	0.99	0.16	18.14	0.0779	0.0020	1.561	0.405
	3.7	0.829	0.827	1.44	0.24	1.53	1.46	1.11	0.14	22.32	0.0959	0.0023	1.301	0.266

Station	Depth	^{231}Pa	^{231}Pa	$^{231}Pa_{corr}$	2se	^{230}Th	^{230}Th	$^{230}Th_{corr}$	2se	^{232}Th	^{232}Th	2se	$^{231}Pa/^{230}Th$	2se
	m	fg/kg	fg/kg	µBq/kg		fg/kg	fg/kg	µBq/kg		pg/kg	pmol/kg			
64	2466.8	0.759	0.756	1.32	0.19	3.24	3.16	2.40	0.14	25.71	0.1104	0.0025	0.551	0.087
59.07°N	2423.6	0.828	0.825	1.44	0.20	3.71	3.62	2.76	0.18	26.12	0.1122	0.0027	0.523	0.080
46.08°W	2374	0.958	0.955	1.67	0.19	3.76	3.68	2.80	0.13	27.16	0.1166	0.0025	0.597	0.074
	2226.6	1.051	1.048	1.83	0.27	5.33	5.24	3.99	0.15	29.28	0.1257	0.0028	0.460	0.070
	1775.6	1.155	1.152	2.01	0.20	5.50	5.38	4.10	0.17	34.64	0.1488	0.0038	0.491	0.054
	890	1.112	1.106	1.93	0.19	4.56	4.39	3.34	0.19	53.17	0.2283	0.0045	0.579	0.066
	395.2	0.898	0.894	1.56	0.17	3.61	3.48	2.65	0.18	40.79	0.1752	0.0110	0.590	0.074
	247.4	0.923	0.918	1.60	0.26	3.23	3.10	2.36	0.18	40.00	0.1718	0.0038	0.680	0.122
	99.2	1.044	1.039	1.81	0.23	3.45	3.30	2.51	0.16	46.12	0.1981	0.0041	0.723	0.105
	29.5	0.963	0.960	1.68	0.28	2.18	2.08	1.58	0.14	30.23	0.1298	0.0029	1.060	0.200
	5.1	0.768	0.766	1.34	0.21	1.54	1.46	1.11	0.17	23.73	0.1019	0.0024	1.202	0.269
69	3676.5	0.404	0.402	0.70	0.10	1.94	1.88	1.43	0.21	19.60	0.0842	0.0025	0.491	0.099
55.84°N	3637.3	0.336	0.334	0.58	0.12	1.92	1.86	1.41	0.16	19.15	0.0822	0.0023	0.414	0.098
48.09°W	3589.5	0.438	0.436	0.76	0.11	2.15	2.08	1.58	0.19	21.39	0.0919	0.0024	0.482	0.091
	3444.7	0.528	0.525	0.92	0.11	3.58	3.49	2.65	0.19	27.76	0.1192	0.0028	0.346	0.048
	2951.8	0.581	0.578	1.01	0.11	5.75	5.64	4.29	0.23	33.80	0.1452	0.0032	0.235	0.029
	2462.6	0.604	0.599	1.05	0.11	6.44	6.31	4.80	0.21	39.48	0.1696	0.0037	0.218	0.025
	2168.1	0.855	0.850	1.49	0.12	6.03	5.90	4.49	0.22	40.95	0.1759	0.0039	0.331	0.031
	1481.3	0.670	0.661	1.16	0.10	4.98	4.73	3.60	0.20	79.22	0.3402	0.0066	0.321	0.033
	989	0.729	0.723	1.26	0.11	4.53	4.35	3.31	0.21	57.18	0.2456	0.0049	0.382	0.041
	445.6	0.692	0.686	1.20	0.07	4.23	4.05	3.08	0.23	55.48	0.2383	0.0047	0.389	0.037
	248.8	0.604	0.598	1.04	0.07	4.06	3.87	2.95	0.18	59.43	0.2552	0.0052	0.355	0.033
	99.5	0.513	0.507	0.89	0.10	3.58	3.40	2.58	0.22	56.06	0.2408	0.0049	0.343	0.047
	28.7	0.554	0.550	0.96	0.07	1.50	1.40	1.07	0.24	30.11	0.1293	0.0029	0.903	0.210
	8.2	0.457	0.453	0.79	0.07	1.42	1.31	0.99	0.17	34.28	0.1472	0.0031	0.797	0.153

Station	Depth	^{231}Pa	^{231}Pa	$^{231}Pa_{corr}$	2se	^{230}Th	^{230}Th	$^{230}Th_{corr}$	2se	^{232}Th	^{232}Th	2se	^{231}Pa/^{230}Th	2se
	m	fg/kg	fg/kg	µBq/kg		fg/kg	fg/kg	µBq/kg		pg/kg	pmol/kg			
77	2487.5					4.02	3.93	2.99	0.14	29.43	0.1264	0.0026		
53°N	2462.8	1.261	1.258	2.20	0.15	4.07	3.97	3.02	0.14	30.06	0.1291	0.0026	0.728	0.059
51.10°W	2414.2	1.113	1.110	1.94	0.10	4.09	4.00	3.04	0.15	29.56	0.1270	0.0026	0.638	0.044
	2268.5	0.989	0.985	1.72	0.12	6.11	6.00	4.56	0.16	33.99	0.1460	0.0030	0.377	0.029
	2170.5	1.355	1.352	2.36	0.13	5.32	5.22	3.97	0.17	30.77	0.1322	0.0028	0.595	0.041
	1678.1	1.267	1.263	2.21	0.13	5.48	5.36	4.08	0.16	37.02	0.1590	0.0031	0.541	0.039
	1235.4	0.580	0.576	1.01	0.13	5.36	5.22	3.97	0.18	44.75	0.1922	0.0037	0.253	0.035
	989.6	1.772	1.767	3.09	0.23	4.96	4.79	3.64	0.17	53.23	0.2286	0.0041	0.848	0.073
	496.4					4.33	4.15	3.16	0.17	55.68	0.2391	0.0044		
	297.9	0.501	0.494	0.86	0.07	4.71	4.50	3.42	0.23	64.41	0.2766	0.0055	0.252	0.026
	78.8	1.200	1.193	2.08	0.14	3.50	3.29	2.50	0.20	65.47	0.2812	0.0053	0.834	0.086
	2.5	0.926	0.923	1.61	0.12	1.34	1.25	0.95	0.17	28.01	0.1203	0.0026	1.699	0.332

^{230}Th and ^{231}Pa are dissolved ^{230}Th and ^{231}Pa activities corrected for the ingrowth from seawater ^{234}U and ^{235}U, respectively, since the time of collection following equations:

$$^{230}Th = {}^{230}Th_m - {}^{234}U \times \left(1 - \exp\left(-\lambda_{^{230}Th} \times t\right)\right) \quad (1)$$

$$^{231}Pa = {}^{231}Pa_m - {}^{235}U \times \left(1 - \exp\left(-\lambda_{^{231}Pa} \times t\right)\right) \quad (2)$$

^{230}Th and ^{231}Pa are further corrected for detrital, U-supported ^{230}Th and ^{231}Pa concentrations as follows:

$$^{230}Th_{corr} = {}^{230}Th_m - (0.6 \times {}^{232}Th_m) \quad (3)$$

$$^{231}Pa_{corr} = {}^{231}Pa_m - 0.046 \times (0.6 \times {}^{232}Th_m) \quad (4)$$

where $^{230}Th_m$, $^{231}Pa_m$ and $^{232}Th_m$ are activities obtained from measurement; ^{235}U and ^{234}U are their average activities in seawater, 1824 µBq/kg (or 112 dpm/1000l) and 45551µBq/kg (or 2801 dpm/1000l,) respectively, obtained from ^{238}U activity of 39610 µBq/kg (or 2436 dpm/1000l) at salinity of 35 (Owens et al., 2011) and assuming natural ^{238}U/^{235}U abundance ratio of 137.88 and seawater ^{234}U/^{238}U activity ratio of 1.15; $\lambda_{^{230}Th}$ and $\lambda_{^{231}Pa}$ are decay constants of ^{230}Th and ^{231}Pa; t is the time between sample collection and chemical separation of U from ^{231}Pa and ^{230}Th. 0.6 is the average ^{238}U/^{232}Th activity ratio in detrital material in the Atlantic (Henderson and Anderson, 2003) and 0.046 represents ^{235}U/^{238}U activity ratio in seawater (Anderson et al., 1990). Half-lives for ^{231}Pa, ^{230}Th and ^{232}Th are 32,760 yr, 75,584 yr and 1.40×10^{10} yr (Cheng et al., 2013; Holden, 1990; Robert et al., 1969).

All errors are 2 standard errors (2se) and include the contribution from sample weighing, spike calibration, ^{231}Pa, ^{230}Th and ^{232}Th in the respective ^{233}Pa and ^{230}Th spikes, blank correction, internal precision and related corrections of mass spectrometric measurement.

S2. CFC-based Age determination

CFC measurement are not available for the GEOVIDE cruise itself. However, with the availability of CFC measurements from OVIDE section in 2012 and water mass composition estimated using extended optimum multi-parameter (eOMP) analysis for both OVIDE and GEOVIDE sections, CFC-based ages can be derived for GEOVIDE section.

1. CFC measurements were available along OVIDE section in 2012 (OVIDE/CATARINA cruise) (de la Paz et al., 2017). This allows the computing of the mean age of water masses using transient time distribution (TTD) method. A more detailed description of TTD method is given in other studies (e.g. Steinfeldt et al., 2009; Waugh et al., 2003). It is important to note that this mean age (referred to as CFC-based age hereafter and in the manuscript) is different from the age calculated based on atmospheric history of CFC (referred to as CFC apparent age hereafter), and therefore is not limited by the time span of the presence of CFC in the atmosphere and inherently deals with age bias due to water mass mixing in CFC apparent age.

Combining CFC-based ages computed with the TTD method for each water sample with water mass composition estimated using eOMP analysis for OVIDE section in 2012 (García-Ibáñez et al., 2015), CFC-based age was calculated for each Source Water Type (SWT) defined in García-Ibáñez et al., 2015 by the equations,

$$\log\,[\text{CFC–based age}]^j = \sum_{i=1}^{12} SWT_i^j \times (log[\text{CFC–based age}]_i) + \varepsilon_j \; j = 1 \rightarrow 424 \; samples \quad (5)$$

$$[\text{CFC} - \text{Age}]^j = \text{anti}\log\,[\text{CFC} - \text{Age}]^j \quad (6)$$

where SWT_i^j is the fraction of SWT *"i"* to sample *"j"* (obtained through the eOMP analysis); $[\text{CFC–based age}]^j$ is CFC-based age for each water sample computed with TTD method along OVIDE section 2012; and ε_j is the residual, representing the portion of CFC–based age that can not be modelled by mixing of SWTs, i.e. the difference between $\log\,[\text{CFC–based age}]^j$ and that obtained as the sum of the contributions by mixing of the individual SWT, $\sum_{i=1}^{12} SWT_i^j \times (log[\text{CFC–based age}]_i)$.

The output of log[CFC-based age]$_i$ and its inversion ([CFC-age]$_i$) is given in Table S2. The squared correlation coefficient (r^2) and standard deviation of the residual, ε_j, are 0.94 and 0.12, respectively.

2. CFC-based age for GEOVIDE section was then calculated employing equation (5) with water mass composition estimated using eOMP analysis along GEOVIDE section (García-Ibáñez et al., 2018) and the output of CFC-based age for SWT (Table S2).

Table S2 Output of log(CFC-age) and the inversion [CFC-age]$_I$ (i.e. CFC-based age) for source water types (SWT)

	log(CFC-age)	CFC-based age
ENACW$_{16}$	1.05±0.20	11±5
ENACW$_{12}$	1.11±0.03	13±1
SPMW$_8$	1.69±0.04	49±5
SAIW	1.19±0.07	16±3
SPMW$_7$	1.26±0.05	18±2
IrSPMW	0.98±0.03	10±1
LSW	1.54±0.02	35±1
MW	1.96±0.04	91±8
PIW	1.33±0.15	22±8
DSOW	1.22±0.07	17±3
ISOW	1.70±0.03	50±4
NEADW$_L$	3.00±0.02	989±48
r^2	0.94	0.943
std(Resid)	0.12	41

ENACW$_{16}$ and ENACW$_{12}$ = East North Atlantic Central Water of 16ºC and 12ºC; SPMW$_8$, SPMW$_7$, IrSPMW = Subpolar Mode Water of 8ºC, 7ºC and of the Irminger Sea; SAIW = Subarctic Intermediate Water; MW = Mediterranean Water; PIW = Polar Intermediate Water; ISOW=Iceland–Scotland Overflow Water; LSW=Labrador Sea Water; DSOW: Denmark Strait Overflow Waters; and NEADW$_L$: Lower North East Atlantic Deep Water. r^2 and std (Resid) represents the squared correlation coefficient and standard deviation of the residual, ε_j, i.e. the difference between log [CFC–based age]^j and that obtained as the sum of the contributions by mixing of the individual SWT, $\sum_{i=1}^{12} SWT_i^j \times (log[\text{CFC–based age}]_i)$.

S3. Scavenging-mixing model and parameterization

A more detailed description of the scavenging-mixing model used in this this study is given in Moran et al. (1997). Briefly, the model takes into account reversible scavenging of the nuclides and water mass mixing. It describes the evolution of nuclides through time in a one-dimensional system, an ocean water column. In the Atlantic, the system is assumed to start at time t=0 in the far North Atlantic and moves southward with time. Transport of material downward relative to the direction of water flow is permitted, to represent the effect of scavenging of radionuclides by sinking particles. Lateral exchange with water outside of the system is not permitted.

The equations to derive the dissolved concentration of each nuclide follows those of Moran et al., (1997). Dissolved concentration of the nuclide is given by,

$$c_d = \frac{C_{pre,t} + P \quad \tau_w}{(K_d\ SPM+1)} \times [1 - \exp(-\frac{(K_d\ SPM+1)}{SK_d\ \tau_w SPM} \times z)] \quad (7)$$

where C_d is the dissolved concentration of the nuclide ; P is the production rate of ^{230}Th and ^{231}Pa, 0.42 µBq/kg/yr (or 2.57 × 10^{-2} dpm/1000l/yr) and 0.039 µBq/kg/yr (or 2.37 × 10^{-3} dpm/1000l/yr), respectively; K_d is the distribution coefficient of the nuclide; λ is the decay constant of the nuclide; $C_{pre,t}$ is the preformed total concentration of ^{230}Th (or ^{231}Pa); SPM is the suspended particle concentration; and S is the particle settling speed, which represents the net effect of particle sinking, disaggregation and aggregation; τ_w is water mass age; z is the water depth.

Initial parameterization was conducted using S=500-1000 m/yr, K_d^{Th}= 1× 10^7 ml/g, K_d^{Pa}= 5× 10^5 ml/g, SPM= 20-50 µg/l, for preformed concentrations set at 0 and surface average from GEOVIDE, i.e., $C_{pre}^{Th} = C_{surface\ average}^{Th}$ = 1.66 µBq/kg, C_{pre}^{Pa}=$C_{surface\ average}^{Pa}$ = 1.31 µBq/kg. With τ_w known from CFC measurements for every depth where ^{230}Th and ^{231}Pa was measured along GEOVIDE section, water-column profiles of both nuclides were simulated for GEOVIDE Station 13 and the parameters were adjusted for the best fit between the simulated and observed profiles (Fig. S1). This gives us the optimized parameters for the analysis in discussion section 4.3, which are listed in Table S3. Our optimized parameters are consistent with values reported by other studies (also listed in Table S3).

Adopting the optimized parameters and setting preformed component (C_{pre}) equal to the nuclide concentrations observed in the upper 100 m of the GEOVIDE section, the modelled evolution of nuclide concentrations with age between 0-500 years at 2000 m and 3500 m water depths, together with GEOVIDE data, is plotted in Figure S2.

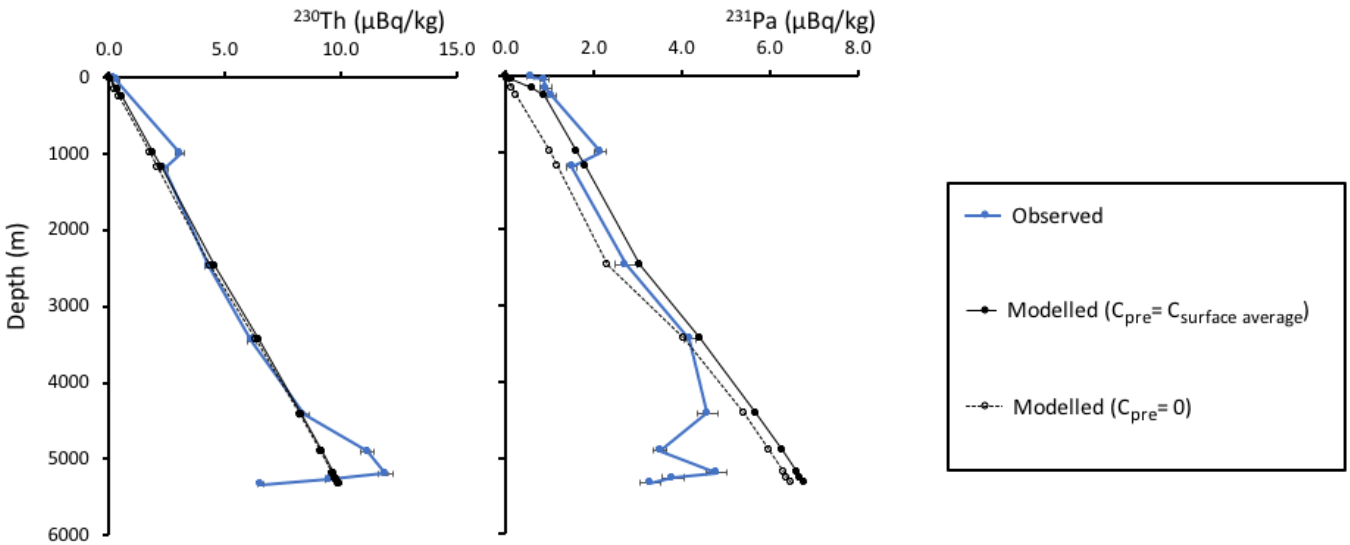

Figure S1: Modelled (dashed black lines) profiles with preformed value set at 0 and surface average concentration from GEOVIDE, and observed (solid blue lines) profiles of Station 13 from GEOVIDE section. The best fit was first sought for ^{230}Th, which gives us the optimized parameters S, SPM and K_d^{Th}. These parameters were then adopted for the simulation of ^{231}Pa profiles, adjusting only K_d^{Pa} to obtain the best fit.

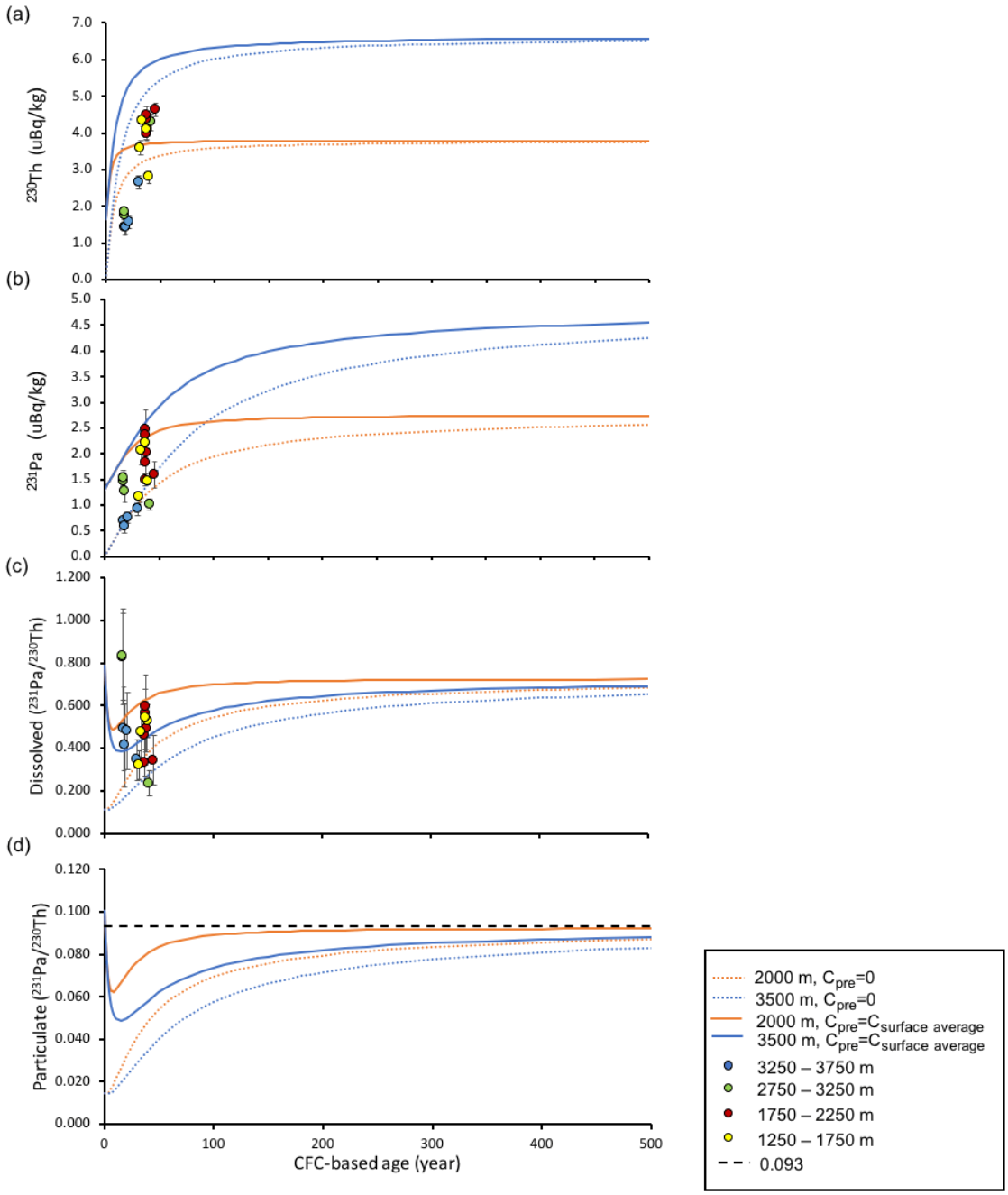

Figure S2: Results from a scavenging-mixing model of ^{230}Th, ^{231}Pa, dissolved ^{231}Pa/^{230}Th and particulate ^{231}Pa/^{230}Th compared to observations. Preformed concentration (C_{pre}) were set at 0 (dashed line) and at the average surface concentration ($C_{surface\ average}$) from GEOVIDE section (solid line), i.e. ^{230}Th= 1.66 µBq/kg, ^{231}Pa= 1.31 µBq/kg.

Table S3 Parameterization of the scavenging-mixing model

	This study	Literature
S (m/yr)	800	500-1000 (Moran et al., 1997)
SPM (μg/l)	25	30 (Labrador Sea, Brewer et al., 1976)
K_d^{Th} (ml/g)	1.1×10^7	1.1×10^7 (Moran et al., 1997)
K_d^{Pa} (ml/g)	1.4×10^6	2.2×10^5 (pure carbonate)~1.4×10^6 g/g (pure opal) (pseudo-K_d, Chase et al., 2002)

S4. Meridional transport of ^{230}Th and ^{231}Pa in the Atlantic

Table S4 Mass balance calculation of meridional transport of ^{230}Th and ^{231}Pa in the Atlantic

	Net meridional transport		Volume of seawater between two latitudes	Production in water column		Removal to sediment		Removal/Production	
	$\times 10^{10}$ μBq/s		$\times 10^{17}$ m^3	$\times 10^{10}$ μBq/s		$\times 10^{10}$ μBq/s		%	
	^{230}Th	^{231}Pa		^{230}Th	^{231}Pa	^{230}Th	^{231}Pa	^{230}Th	^{231}Pa
GEOVIDE-4.5°S	-7.76	-4.75	1.48	200.8	18.6	193.1	13.8	96.2	74.2
4.5°S-45°S	0.33	0.017	1.02	138.4	12.8	138.7	12.8	99.8	100.0

Positive value indicates northward transport; negative value indicates southward transport. Production rate of ^{230}Th and ^{231}Pa in water column are 0.42 and 0.039 μBq/kg/yr, respectively.

References

Anderson, R. F., Lao, Y., Broecker, W. S., Trumbore, S. E., Hofmann, H. J. and Wolfli, W.: Boundary scavenging in the Pacific Ocean: a comparison of ^{10}Be and ^{231}Pa, Earth Planet. Sci. Lett., 96(3), 287–304, doi:https://doi.org/10.1016/0012-821X(90)90008-L, 1990.

Brewer, P. G., Spencer, D. W., Biscaye, P. E., Hanley, A., Sachs, P. L., Smith, C. L., Kadar, S. and Fredericks, J.: The distribution of particulate matter in the Atlantic Ocean, Earth Planet. Sci. Lett., 32(2), 393–402, doi:https://doi.org/10.1016/0012-821X(76)90080-7, 1976.

Chase, Z., Anderson, R. F., Fleisher, M. Q. and Kubik, P. W.: The influence of particle composition and particle flux on

scavenging of Th, Pa and Be in the ocean, Earth Planet. Sci. Lett., 204(1), 215–229, doi:https://doi.org/10.1016/S0012-821X(02)00984-6, 2002.

Cheng, H., Lawrence Edwards, R., Shen, C.-C., Polyak, V. J., Asmerom, Y., Woodhead, J., Hellstrom, J., Wang, Y., Kong, X., Spötl, C., Wang, X. and Calvin Alexander, E.: Improvements in ^{230}Th dating, ^{230}Th and ^{234}U half-life values, and U–Th isotopic measurements by multi-collector inductively coupled plasma mass spectrometry, Earth Planet. Sci. Lett., 371, 82–91, doi:10.1016/j.epsl.2013.04.006, 2013.

García-Ibáñez, M. I., Pardo, P. C., Carracedo, L. I., Mercier, H., Lherminier, P., Ríos, A. F. and Pérez, F. F.: Structure, transports and transformations of the water masses in the Atlantic Subpolar Gyre, Prog. Oceanogr., 135, 18–36, doi:https://doi.org/10.1016/j.pocean.2015.03.009, 2015.

García-Ibáñez, M. I., Pérez, F. F., Lherminier, P., Zunino, P., Mercier, H. and Tréguer, P.: Water mass distributions and transports for the 2014 GEOVIDE cruise in the North Atlantic, Biogeosciences, 15(7), 2057–2090 [online] Available from: https://doi.org/10.5194/bg-15-2075-2018, 2018.

Henderson, G. M. and Anderson, R. F.: The U-series Toolbox for Paleoceanography, Rev. Mineral. Geochemistry, 52(1), 493–531 [online] Available from: http://dx.doi.org/10.2113/0520493, 2003.

Holden, N. E.: Total half-lives for selected nuclides, Pure Appl. Chem., 62, 941, doi:10.1351/pac199062050941, 1990.

de la Paz, M., García-Ibáñez, M. I., Steinfeldt, R., Ríos, A. F. and Pérez, F. F.: Ventilation versus biology: What is the controlling mechanism of nitrous oxide distribution in the North Atlantic?, Global Biogeochem. Cycles, 31(4), 745–760, doi:10.1002/2016GB005507, 2017.

Moran, S. B., Charette, M. A., Hoff, J. A. and Edwards, R. L.: Distribution of 230Th in the Labrador Sea and its relation to ventilation, Earth Planet. Sci. Lett., 150, 151–160, 1997.

Owens, S. A., Buesseler, K. O. and Sims, K. W. W.: Re-evaluating the 238U-salinity relationship in seawater: Implications for the 238U–234Th disequilibrium method, Mar. Chem., 127(1), 31–39, doi:https://doi.org/10.1016/j.marchem.2011.07.005, 2011.

Robert, J., Miranda, C. F. and Muxart, R.: Mesure de la période du protactinium 231 par microcalorimétrie, Radiochim. Acta, 11(2), 104–108, doi:10.1524/ract.1969.11.2.104, 1969.

Steinfeldt, R., Rhein, M., Bullister, J. L. and Tanhua, T.: Inventory changes in anthropogenic carbon from 1997–2003 in the Atlantic Ocean between 20°S and 65°N, Global Biogeochem. Cycles, 23(3), doi:10.1029/2008GB003311, 2009.

Waugh, D. W., Hall, T. M. and Haine, T. W. N.: Relationships among tracer ages, J. Geophys. Res., 108(C5), 3138, doi:10.1029/2002JC001325, 2003.